Journal , manuscript No.
(will be inserted by the editor)

Numerical test of Schoenberg-Muir averaging theory

Short title: Schoenberg-Muir theory.

José M. Carcione [1] · **Stefano Picotti**[1], **Fabio Cavallini**[1] · **Juan E. Santos**[2]

This paper is dedicated to the memory of Michael A. Schoenberg.

Abstract The Schoenberg-Muir theory states that an equivalent, homogeneous and anisotropic medium can be constructed from a layered medium composed of several thin layers, each anisotropic, under the assumption of stationarity. To test the theory we consider single transversely isotropic layers with different orientations of the symmetry axis and perform numerical simulations of wave propagation with a full-wave solver. The equivalent media have orthorhombic and monoclinic symmetries. It is shown that the theory performs very well from the kinematical and dynamical points of view, even for strong anisotropy

Keywords Schoenberg-Muir theory · thin layers · fractures · cracks · anisotropy · numerical modeling.

1 Introduction

Thin transversely isotropic layers (with a vertical symmetry axis) (VTI media) behave as a homogeneous transversely isotropic medium when the wavelength is much longer than the ticknesses. To our knowledge, the first to study the problem using isotropic layers was Bruggeman (1937). Other investigators analyzed the problem using different approaches, e.g., Riznichenko (1949) and Postma (1955), who considered a two-constituent periodically layered medium. Later, Backus (1962) showed that periodicity is not necessary and also obtained the average elasticity constants in the more general case when the single layers are transversely isotropic with the symmetry axis perpendicular to the layering plane. He assumed stationarity, i.e., in a given length of composite medium much smaller than the wavelength, the proportion of each material is constant.

[1]
Istituto Nazionale di Oceanografia e di Geofisica Sperimentale (OGS), Borgo Grotta Gigante 42c, 34010 Sgonico, Trieste, Italy.
E-mail: jcarcione@inogs.it [1]
Departamento de Geofísica Aplicada, Fac. Ciencias Astronómicas y Geofísicas, UNLP, Paseo del Bosque S/N, La Plata, 1900, Argentina.
E-mail: santos@math.purdue.edu

Schoenberg and Muir (1989) extended Backus approach to single layers of arbitrary anisotropic layers using a matrix formalism. However, this generalization has been questioned by Hudson and Crampin (1991), who argue that the theory cannot be applied to oblique sets of layers or cracks (even for weak anisotropy), since the structure is no longer one-dimensional and Backus's assumptions are invalidated.

Backus averaging has been verified numerically by Carcione et al. (1991), who found that the minimum ratio between the P-wave dominant pulse wavelength and the spatial period of the layering depends on the contrast between the constituents. For instance, for a periodic sequence of epoxy-glass it is around 8, and for sandstone-limestone (which has a lower reflection coefficient) it is between 5 and 6. In any case, an optimal ratio can be found for which the equivalence between a finely layered medium and a homogeneous transversely isotropic medium is valid. In this work, we consider a periodic sequence of VTI-ψTI layers, where ψTI is the VTI medium rotated by an angle ψ. In particular, we consider $\psi = \pi/2$ and $\pi/4$. The resulting equivalent media have orthorhombic and monoclinic symmetries, respectively.

We compute the wave field with a modeling method used by Carcione et al. (1991), generalized to the anisotropic case. Details of this space-time domain direct method can be found in Carcione et al. (1988, 1992).

2 Schoenberg-Muir theory

Let us consider a finely layered medium composed of N layers of arbitrary anisotropy (Figure 1), with the z-axis perpendicular to the layering plane. Each layer is defined by the density ρ, the proportion p_n and the elastic constants c_{IJ}. The stress-strain relation of each layer can written as

$$\begin{pmatrix} \sigma_1 \\ \sigma_2 \\ \sigma_6 \\ \\ \sigma_3 \\ \sigma_4 \\ \sigma_5 \end{pmatrix} = \begin{pmatrix} \sigma_{11} \\ \sigma_{22} \\ \sigma_{12} \\ \\ \sigma_{33} \\ \sigma_{23} \\ \sigma_{13} \end{pmatrix} = \begin{pmatrix} c_{11}\ c_{12}\ c_{16} & c_{13}\ c_{14}\ c_{15} \\ c_{12}\ c_{22}\ c_{26} & c_{23}\ c_{24}\ c_{25} \\ c_{16}\ c_{26}\ c_{66} & c_{36}\ c_{46}\ c_{56} \\ & \\ c_{13}\ c_{23}\ c_{36} & c_{33}\ c_{34}\ c_{35} \\ c_{14}\ c_{24}\ c_{46} & c_{34}\ c_{44}\ c_{45} \\ c_{15}\ c_{25}\ c_{56} & c_{35}\ c_{45}\ c_{55} \end{pmatrix} \begin{pmatrix} e_1 \\ e_2 \\ e_6 \\ \\ e_3 \\ e_4 \\ e_5 \end{pmatrix}, \tag{1}$$

where σ_I denotes stress component and e_I denotes strain component in the Voigt notation (e.g., Carcione, 2007). The stiffness matrix involved in equation (1) can be rewritten in terms of four submatrices as

$$\begin{pmatrix} C_{TT} & C_{TN} \\ \\ C_{TN}^{\top} & C_{NN} \end{pmatrix}. \tag{2}$$

According to Schoenberg and Muir (1989), the equivalent homogeneous medium is defined by the following matrix:

$$\begin{pmatrix} \bar{C}_{TT} & \bar{C}_{TN} \\ \\ \bar{C}_{TN}^{\top} & \bar{C}_{NN} \end{pmatrix}, \tag{3}$$

where

$$\begin{aligned}\bar{C}_{NN} &= \langle C_{NN}^{-1}\rangle^{-1},\\ \bar{C}_{TN} &= \langle C_{TN}C_{NN}^{-1}\rangle\bar{C}_{NN},\\ \bar{C}_{TT} &= \langle C_{TT}\rangle - \langle C_{TN}C_{NN}^{-1}C_{NT}\rangle + \bar{C}_{TN}\langle C_{NN}^{-1}C_{NT}\rangle,\end{aligned} \tag{4}$$

where the thickness weighted average of a quantity C is defined as

$$\langle C\rangle = \sum_{n=1}^{N} p_n\ C_n. \tag{5}$$

In this work, we consider periodic systems of equal composition whose single layers have transversely isotropic symmetry (VTI) or rotated versions of this medium, ψTI, where ψ is the rotation angle. Specifically, we consider VTI = 0TI, 90TI = HTI and 45TI media as shown in Figure 1. The new elasticity matrix after rotation of a medium is given in Appendix A.

The equivalent elasticity matrices for VTI-HTI and VTI-45TI periodic systems are given in Appendix B, where $p_1 = p_2 = 1/2$ and HTI and 45VTI indicate the same VTI medium whose symmetry axis is rotated by the angles $\psi = \pi/2$ and $\psi = \pi/4$, respectively.

3 Time-domain modeling in monoclinic media

We consider the symmetry plane of a monoclinic medium, say, the (x, z)-plane, and recast the equation of motion in the particle-velocity/stress formulation (Carcione, 2007). In this plane, we identify two sets of uncoupled differential equations

$$\begin{aligned}\dot{v}_1 &= \rho^{-1}\left(\partial_1\sigma_{11} + \partial_3\sigma_{13} + f_1\right)\\ \dot{v}_3 &= \rho^{-1}\left(\partial_1\sigma_{13} + \partial_3\sigma_{33} + f_3\right)\\ \dot{\sigma}_{11} &= c_{11}\partial_1 v_1 + c_{13}\partial_3 v_3 + c_{15}(\partial_1 v_3 + \partial_3 v_1)\\ \dot{\sigma}_{33} &= c_{13}\partial_1 v_1 + c_{33}\partial_3 v_3 + c_{35}(\partial_1 v_3 + \partial_3 v_1)\\ \dot{\sigma}_{13} &= c_{15}\partial_1 v_1 + c_{35}\partial_3 v_3 + c_{55}(\partial_1 v_3 + \partial_3 v_1)\end{aligned} \tag{6}$$

and

$$\begin{aligned}\dot{v}_2 &= \rho^{-1}\left(\partial_1\sigma_{12} + \partial_3\sigma_{23} + f_2\right)\\ \dot{\sigma}_{23} &= c_{44}\partial_3 v_2 + c_{46}\partial_1 v_2\\ \dot{\sigma}_{12} &= c_{46}\partial_3 v_2 + c_{66}\partial_1 v_2,\end{aligned} \tag{7}$$

where v_i are the particle-velocity components, ρ is the density, f_i are external forces, a dot above a variable denotes time differentiation and ∂_i indicates the spatial partial derivative with respect to the variable x_i. The strain vector and the particle-velocity components are related as

$$\begin{pmatrix}\dot{e}_1\\ \dot{e}_2\\ \dot{e}_3\\ \dot{e}_4\\ \dot{e}_5\\ \dot{e}_6\end{pmatrix} = \begin{pmatrix}\partial_1 v_1\\ \partial_2 v_2\\ \partial_3 v_3\\ \partial_2 v_3 + \partial_3 v_2\\ \partial_1 v_3 + \partial_3 v_1\\ \partial_1 v_2 + \partial_2 v_1\end{pmatrix}. \tag{8}$$

The first set of equations (6) describes in-plane particle motion while the second set (7) describes cross-plane particle motion, that is, the propagation of a pure shear wave. The

uncoupling implies that a cross-plane shear wave exists at a plane of mirror symmetry. The plan-wave analysis, including the calculation of the phase group velocities, is given in Appendix C.

The numerical algorithm used to solve the equation of motion is based on the Fourier pseudospectral method for computing the spatial derivatives and a 4th-order Runge-Kutta technique for calculating the wavefield recursively in time (e.g., Carcione, 2007).

4 Simulations

We consider the qP-qS case and

$$\begin{pmatrix} c_{11} & c_{13} & c_{15} \\ c_{13} & c_{33} & c_{35} \\ c_{15} & c_{35} & c_{55} \end{pmatrix} = \begin{pmatrix} 46 & 18 & 0 \\ 18 & 30 & 0 \\ 0 & 0 & 7 \end{pmatrix}, \tag{9}$$

in GPa. In this case, c_{12} need not to be specified, since it has not influence on the results. The anisotropy coefficient of the medium defined by the elasticity matrix (9) is 50 $(c_{11} - c_{33})/c_{33} = 26$ %.

According to equations (18) and (22), rotations of $\pi/2$ and $\pi/4$ yield

$$\begin{pmatrix} 30 & 18 & 0 \\ 18 & 46 & 0 \\ 0 & 0 & 7 \end{pmatrix} \quad \text{and} \quad \begin{pmatrix} 35 & 21 & -4 \\ 21 & 35 & -4 \\ -4 & -4 & 10 \end{pmatrix}, \tag{10}$$

respectively. From equations (21) and (23), the effective VTI-HTI and VTI-45TI media have the following elasticity matrices:

$$\begin{pmatrix} 38 & 18 & 0 \\ 18 & 36.3 & 0 \\ 0 & 0 & 7 \end{pmatrix} \quad \text{and} \quad \begin{pmatrix} 40 & 19 & -1.6 \\ 19 & 31.9 & -1.5 \\ -1.6 & -1.5 & 8.1 \end{pmatrix}, \tag{11}$$

respectively. We take $\rho = 2600$ kg/m^3. Figure 2 shows the group (energy) velocity curves corresponding to the orthorhombic (a) and monoclinic (b) effective media. The VTI medium is rotated to obtain the HTI (45TI) medium and then the VTI and HTI (45TI) are averaged to obtain the effective orthorhombic (VTI-HTI) and monoclinic (VTI-47TI) media.

The source used in the simulations is a vertical force (f_1) with the following time history:

$$h(t) = \left(u - \frac{1}{2}\right)\exp(-u), \quad u = \left[\frac{\pi(t - t_s)}{t_p}\right]^2, \tag{12}$$

where t_p is the period of the wave, $f_p = 1/t_p$ is the central frequency and we take $t_s = 1.4t_p$.

The simulations use a 455 $\times$ 455 mesh with 1 m grid spacing and the central frequency of the source is $f_p = 80$ Hz. The force is located at the center of the mesh. The Runge-Kutta algorithm has a time step of 0.1 ms and the solution is obtained at a maximum time of 70 ms. The snapshots corresponding to the group-velocity curves shown in Figure 1 are displayed in Figure 3, where it is verified that the modeling code reproduces correctly the predictions of the plane-wave analysis. Figure 4 shows

the snapshots in the orthorhombic (a) and monoclinic (b) effective (Schoenberg-Muir) media (upper pictures). The lower pictures display the simulations in the finely-layered media. As can be seen, the snapshots are indistinguible, indicating that the Schoenberg-Muir theory provides a good approximation to fine layering at long wavelengths.

Figure 5 shows the time history at $(x, z) = (57, 57)$ m from the source location for the VTI-HTI orthorhombic (a) and VTI-45TI monoclinic (b) media. The solid line corresponds to the effective (Schoenberg-Muir) monoclinic medium and the dots to the simulations in the finely-layered medium. As can be seen, the agreement is excellent.

We have also considered a VTI medium defined by

$$\begin{pmatrix} c_{11} & c_{13} & c_{15} \\ c_{13} & c_{33} & c_{35} \\ c_{15} & c_{35} & c_{55} \end{pmatrix} = \begin{pmatrix} 60 & 3 & 0 \\ 3 & 30 & 0 \\ 0 & 0 & 7 \end{pmatrix}, \tag{13}$$

which has an anisotropy coefficient of 50 % (see wavefront in Figure 6) and obtained an excellent match between the results of the theory and the simulations in layered media, as can be appreciated in Figure 7, where the time history at $(x, z) = (51, 51)$ m from the source location VTI-45TI monoclinic medium is shown.

The theory performs equally well for amplitudes, going beyond the expectancy of the authors also, since they state: "The real limitation is the long-wavelength one, which says, in effect, that it is concerned with kinematics arrival times-alone. It does not address the important dynamical question of how high-frequency energy is lost from the coherent to the scattered field." It is evident in Figures 5 and 7 that at long wavelengths, the theory performs equally well for amplitudes.

5 Conclusions

We performed numerical simulations (snapshots and time histories) of wave propagation in a layered medium whose layers are anisotropic and thin compared to the wavelength, and compared the results to similar simulations in an equivalent medium obtained from the Schoenberg-Muir theory. The assumptions of the theory (Backus's assumptions) state that the model works for small crack aspect ratio, very long flat parallel fractures and fracture spacings spacings and layer thicknesses small compared to the wavelength. Under these conditions, the Schoenberg-Muir theory is valid from the kinematic (traveltimes) and dynamic (amplitudes) point of view, no matter how anisotropic are the single constituent layers. In the case of obliquely aligned cracks (the monoclinic case), the theory performs equally well.

References

1. G. E. Backus, Long-wave elastic anisotropy produced by horizontal layering, J. Geophys. Res. 67 (1962), 4427-4440.
2. D. A. G. Bruggeman, Berechnungen der verschiedener physikalischen Konstanten von heterogenen Substanzen. III: Die elastischen Konstanten der quasi-isotropen Mischkörper aus isotropen Substanzen: Annalen der Physik 29 (1937), 160-178.
3. J. M. Carcione, Wave fields in real media: Wave propagation in anisotropic, anelastic, porous and electromagnetic media, Handbook of Geophysical Exploration, vol. 38, Elsevier (2nd edition, revised and extended), 2007.
4. J. M. Carcione, D. Kosloff, A. Behle, Long wave anisotropy in stratified media: a numerical test, Geophysics 56 (1991), 245-254.
5. J. M. Carcione, D. Kosloff, A. Behle, and G. Seriani, A spectral scheme for wave propagation simulation in 3-D elastic-anisotropic media, Geophysics 57 (1992), 1593-1607.
6. J. M. Carcione, D. Kosloff, and R. Kosloff, Wave propagation simulation in an anisotropic (transversely isotropic) medium, Q. Jl. Mech. Appl. Math. 41 (1988), 320-345.
7. J. A. Hudson, S. Crampin, On: "A calculus for finely layered anisotropic media" by M. Schoenberg and F. Muir (Geophysics, 54, 581-589, May 1989), Geophysics 56 (1991), 575; doi:10.1190/1.1486691.
8. G. W. Postma, Wave propagation in a stratified medium, Geophysics, 20 (1955), 780-806.
9. Y. V. Riznichenko, Seismic quasi-anisotropy, Bull. Acad. Sci. USSR, Geograph. Geophys. Serv. 13 (1949), 518-544.
10. M. Schoenberg, F. Muir, F., A calculus for finely layered media, Geophysics 54 (1989), 581-589.

A Elasticity matrix of a rotated medium

A VTI medium with symmetry axis along the z-axis has the following the stiffness matrix: given by

$$\mathbf{C} = \begin{pmatrix} c_{11} & c_{12} & c_{13} & 0 & 0 & 0 \\ c_{12} & c_{11} & c_{13} & 0 & 0 & 0 \\ c_{13} & c_{13} & c_{33} & 0 & 0 & 0 \\ 0 & 0 & 0 & c_{55} & 0 & 0 \\ 0 & 0 & 0 & 0 & c_{55} & 0 \\ 0 & 0 & 0 & 0 & 0 & c_{66} \end{pmatrix}, \quad 2c_{66} = c_{11} - c_{12}. \tag{14}$$

A clockwise rotation of the vertical symmetry axis through an angle ψ about the y-axis has the orthogonal transformation matrix

$$\begin{pmatrix} \cos\psi & 0 & \sin\psi \\ 0 & 1 & 0 \\ -\sin\psi & 0 & \cos\psi \end{pmatrix}. \tag{15}$$

The corresponding Bond transformation matrix is (Carcione, 2007),

$$\mathbf{M} = \begin{pmatrix} \cos^2\psi & 0 & \sin^2\psi & 0 & \sin(2\psi) & 0 \\ 0 & 1 & 0 & 0 & 0 & 0 \\ \sin^2\psi & 0 & \cos^2\psi & 0 & -\sin(2\psi) & 0 \\ 0 & 0 & 0 & \cos\psi & 0 & -\sin\psi \\ -\frac{1}{2}\sin(2\psi) & 0 & \frac{1}{2}\sin(2\psi) & 0 & \cos(2\psi) & 0 \\ 0 & 0 & 0 & 0 & 0 & \cos\psi \end{pmatrix}. \tag{16}$$

Then, the stiffness matrix with the rotated symmetry axis is given by (Carcione, 2007),

$$\mathbf{C}' = \mathbf{M} \cdot \mathbf{C} \cdot \mathbf{M}^\top. \tag{17}$$

B Effective elasticity matrices for VTI-HTI and VTI-45TI media.

First, we consider a periodic system of VTI and HTI layers, where the HTI medium, labeled 2, is the same VTI medium, labeled 1. Using (17), an angle $\psi = \pi/2$ transforms a VTI medium into an HTI medium,

$$\begin{pmatrix} c_{11} & c_{12} & c_{13} & 0 & 0 & 0 \\ c_{12} & c_{11} & c_{13} & 0 & 0 & 0 \\ c_{13} & c_{13} & c_{33} & 0 & 0 & 0 \\ 0 & 0 & 0 & c_{55} & 0 & 0 \\ 0 & 0 & 0 & 0 & c_{55} & 0 \\ 0 & 0 & 0 & 0 & 0 & c_{66} \end{pmatrix} \rightarrow \begin{pmatrix} c_{33} & c_{13} & c_{13} & 0 & 0 & 0 \\ c_{13} & c_{11} & c_{12} & 0 & 0 & 0 \\ c_{13} & c_{12} & c_{11} & 0 & 0 & 0 \\ 0 & 0 & 0 & c_{66} & 0 & 0 \\ 0 & 0 & 0 & 0 & c_{55} & 0 \\ 0 & 0 & 0 & 0 & 0 & c_{55} \end{pmatrix}. \tag{18}$$

According to equations (1), (3) and (18),

$$C_{TT}^{(1)} = \begin{pmatrix} c_{11} & c_{12} & 0 \\ c_{12} & c_{11} & 0 \\ 0 & 0 & c_{66} \end{pmatrix}, \quad C_{TN}^{(1)} = \begin{pmatrix} c_{13} & 0 & 0 \\ c_{13} & 0 & 0 \\ 0 & 0 & 0 \end{pmatrix}, \quad C_{NN}^{(1)} = \begin{pmatrix} c_{33} & 0 & 0 \\ 0 & c_{55} & 0 \\ 0 & 0 & c_{55} \end{pmatrix}, \tag{19}$$

and

$$C_{TT}^{(2)} = \begin{pmatrix} c_{33} & c_{13} & 0 \\ c_{13} & c_{11} & 0 \\ 0 & 0 & c_{55} \end{pmatrix}, \quad C_{TN}^{(2)} = \begin{pmatrix} c_{13} & 0 & 0 \\ c_{12} & 0 & 0 \\ 0 & 0 & 0 \end{pmatrix}, \quad C_{NN}^{(2)} = \begin{pmatrix} c_{11} & 0 & 0 \\ 0 & c_{66} & 0 \\ 0 & 0 & c_{55} \end{pmatrix}, \tag{20}$$

with $c_{66} = \frac{1}{2}(c_{11} - c_{12})$.

Using equation (3), the effective medium composed of VTI-HTI layers has orthorhombic symmetry and is given by the following symmetric elasticity matrix:

$$\begin{pmatrix} \frac{c_{11}+c_{33}}{2} & \frac{c_{12}+c_{13}}{2} & c_{13} & 0 & 0 & 0 \\ * & c_{11}-\frac{(c_{12}-c_{13})^2}{2(c_{11}+c_{33})} & \frac{c_{11}c_{13}+c_{12}c_{33}}{c_{11}+c_{33}} & 0 & 0 & 0 \\ * & * & \frac{2c_{11}c_{33}}{c_{11}+c_{33}} & 0 & 0 & 0 \\ * & * & * & \frac{2(c_{11}-c_{12})c_{55}}{c_{11}-c_{12}+2c_{55}} & 0 & 0 \\ * & * & * & * & c_{55} & 0 \\ * & * & * & * & * & \frac{1}{4}(c_{11}-c_{12}+2c_{55}) \end{pmatrix}. \tag{21}$$

Now, we consider a periodic system of VTI and 45TI layers, where the 45TI medium, labeled 2, is the same VTI medium, but rotated by 45°. An angle $\psi = \pi/4$ transforms a VTI medium into an 45TI medium, whose (symmetric) elasticity matrix is

$$\begin{pmatrix} a+c_{55} & \frac{1}{2}(c_{12}+c_{13}) & a-c_{55} & 0 & \frac{1}{4}(c_{33}-c_{11}) & 0 \\ * & c_{11} & \frac{1}{2}(c_{12}+c_{13}) & 0 & \frac{1}{2}(c_{13}-c_{12}) & 0 \\ * & * & a+c_{55} & 0 & \frac{1}{4}(c_{33}-c_{11}) & 0 \\ * & * & * & b & 0 & \frac{1}{4}(-c_{11}+c_{12}+2c_{55}) \\ * & * & * & * & \frac{1}{4}(c_{11}-2c_{13}+c_{33}) & 0 \\ * & * & * & * & * & b \end{pmatrix} \tag{22}$$

with

$$\begin{aligned} 4a &= c_{11}+2c_{13}+c_{33}, \\ 4b &= c_{11}-c_{12}+2c_{55}. \end{aligned}$$

Combining the 45TI and VTI media, the effective medium has monoclinic symmetry and is given by the following symmetric elasticity matrix:

$$\begin{pmatrix} \bar{c}_{11} & \bar{c}_{12} & \bar{c}_{13} & 0 & \bar{c}_{15} & 0 \\ * & \bar{c}_{22} & \bar{c}_{23} & 0 & \bar{c}_{25} & 0 \\ * & * & \bar{c}_{33} & 0 & \bar{c}_{35} & 0 \\ * & * & * & \bar{c}_{44} & 0 & \bar{c}_{46} \\ * & * & * & * & \bar{c}_{55} & 0 \\ * & * & * & * & * & \bar{c}_{66} \end{pmatrix}, \tag{23}$$

where

$$
\begin{aligned}
&D\bar{c}_{11} = c_{11}^2(c_{33}+c_{55}) + c_{11}C + c_{33}[-c_{13}^2 + c_{55}(c_{33}+4c_{55})],\\
&D\bar{c}_{12} = c_{13}[c_{33}(-c_{13}+c_{55}) + c_{11}(c_{33}+c_{55})] + c_{12}[C + c_{33}(c_{11}-c_{13}) + c_{55}(c_{11}-c_{33})],\\
&-D\bar{c}_{13} = (c_{13}+c_{33})(c_{13}^2 - c_{11}c_{33}) + 2c_{55}[-c_{13}(c_{11}+3c_{33}) + 2c_{55}(c_{33}-c_{13})],\\
&D\bar{c}_{15} = c_{55}(-c_{11}+c_{33})(c_{13}+c_{33}+2c_{55}),\\
&\bar{c}_{22} = c_{11} - (c_{12}-c_{13})^2(c_{33}+c_{55})D^{-1},\\
&\bar{c}_{23} = c_{13} - c_{33}(c_{12}-c_{13})(c_{13}-c_{33}-2c_{55})D^{-1},\\
&-D\bar{c}_{25} = c_{55}(c_{12}-c_{13})(c_{13}+3c_{33}+2c_{55}),\\
&D\bar{c}_{33} = 2c_{33}[-c_{13}^2 + (c_{11}+2c_{55})(c_{33}+2c_{55})],\\
&D\bar{c}_{35} = 2c_{33}c_{55}(-c_{11}+c_{33}),\\
&F\bar{c}_{44} = 2c_{55}(c_{11}-c_{12}+2c_{55}),\\
&D\bar{c}_{46} = c_{55}(-c_{11}+c_{12}+2c_{55}),\\
&D\bar{c}_{55} = 2c_{55}[-c_{13}^2 + (c_{33}+c_{55})(c_{33}-2c_{13}) + c_{11}(2c_{33}+c_{55})],\\
&4F\bar{c}_{66} = (c_{11}-c_{12})^2 + 4c_{55}[3(c_{11}-c_{12}) + c_{55}],\\
&C = -c_{13}^2 + c_{33}^2 + 6c_{33}c_{55} + 4c_{55}^2,\\
&D = C - 2c_{13}c_{33} + 2c_{11}(c_{33}+c_{55}),\\
&F = c_{11} - c_{12} + 6c_{55}.
\end{aligned}
\tag{24}
$$

C Phase and group velocities of the effective anisotropic medium.

In the symmetry plane of a monoclinic medium there is a pure shear wave and two coupled waves. The respective phase velocity surfaces in the (x,z)-plane are

$$
\begin{aligned}
&\Gamma_{22} - \rho v_p^2 = 0,\\
&(\Gamma_{11} - \rho v_p^2)(\Gamma_{33} - \rho v_p^2) - \Gamma_{13}^2 = 0
\end{aligned}
\tag{25}
$$

and

$$
\begin{aligned}
&\Gamma_{11} = c_{11}l_1^2 + c_{55}l_3^2 + 2c_{15}l_1l_3,\\
&\Gamma_{22} = c_{66}l_1^2 + c_{44}l_3^2 + 2c_{46}l_1l_3,\\
&\Gamma_{33} = c_{33}l_3^2 + c_{55}l_1^2 + 2c_{35}l_1l_3,\\
&\Gamma_{13} = c_{15}l_1^2 + c_{35}l_3^2 + (c_{13}+c_{55})l_1l_3
\end{aligned}
\tag{26}
$$

(Carcione, 2007), where v_p is the phase velocity and $l_1 = \sin\theta$ and $l_3 = \cos\theta$, with θ the phase propagation angle. The SH-wave group velocity is

$$
\mathbf{v}_g = \frac{1}{\rho v_p}[(c_{66}l_1 + c_{46}l_3)\hat{\mathbf{e}}_1 + (c_{44}l_3 + c_{46}l_1)\hat{\mathbf{e}}_3]. \tag{27}
$$

On the other hand, the qP and qS group-velocity components are

$$
v_{g1} = \left(\frac{1}{v_p}\right)\frac{(\Gamma_{33}-\rho v_p^2)(c_{11}l_1 + c_{15}l_3) + (\Gamma_{11}-\rho v_p^2)(c_{55}l_1 + c_{35}l_3) - \Gamma_{13}[2c_{15}l_1 + (c_{13}+c_{55})l_3]}{\rho(\Gamma_{11}+\Gamma_{33}-2\rho v_p^2)} \tag{28}
$$

and

$$
v_{g3} = \left(\frac{1}{v_p}\right)\frac{(\Gamma_{33}-\rho v_p^2)(c_{55}l_3 + c_{15}l_1) + (\Gamma_{11}-\rho v_p^2)(c_{33}l_3 + c_{35}l_1) - \Gamma_{13}[2c_{35}l_3 + (c_{13}+c_{55})l_1]}{\rho(\Gamma_{11}+\Gamma_{33}-2\rho v_p^2)}. \tag{29}
$$

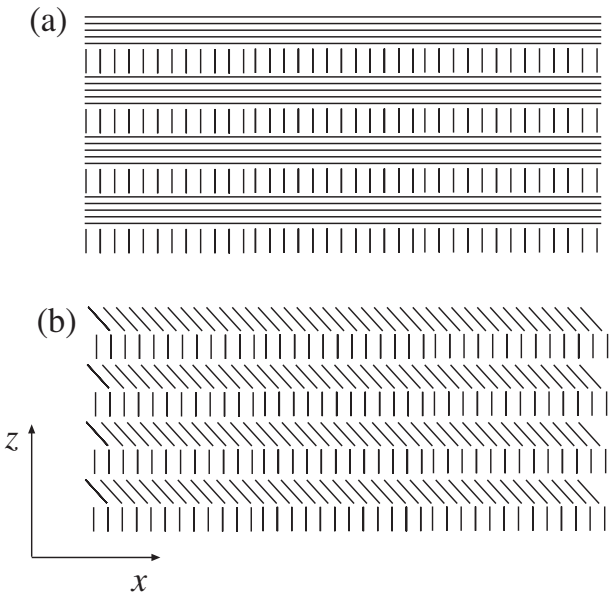

Fig. 1 A stack of thin strata (compared to the wavelength) composed of HTI and VTI layers (a) and 45TI and VTI layers (b). The percentage of each constituent is assumed to be stationary with respect to the vertical coordinate.

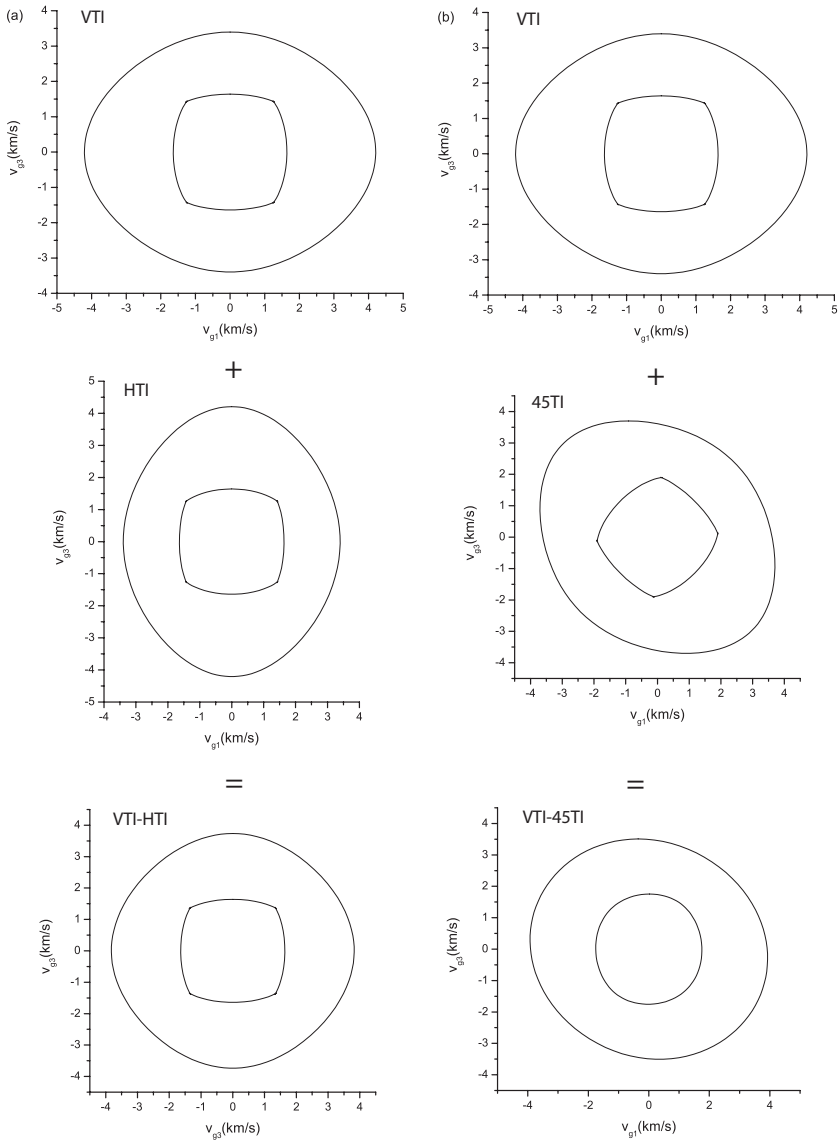

Fig. 2 Group (energy) velocity curves corresponding to the orthorhombic (a) and monoclinic (b) effective media. The VTI medium is rotated to obtain the HTI (45TI) medium and then the VTI and HTI (45TI) are averaged to obtain the effective orthorhombic (VTI-HTI) and monoclinic (VTI-47TI) media.

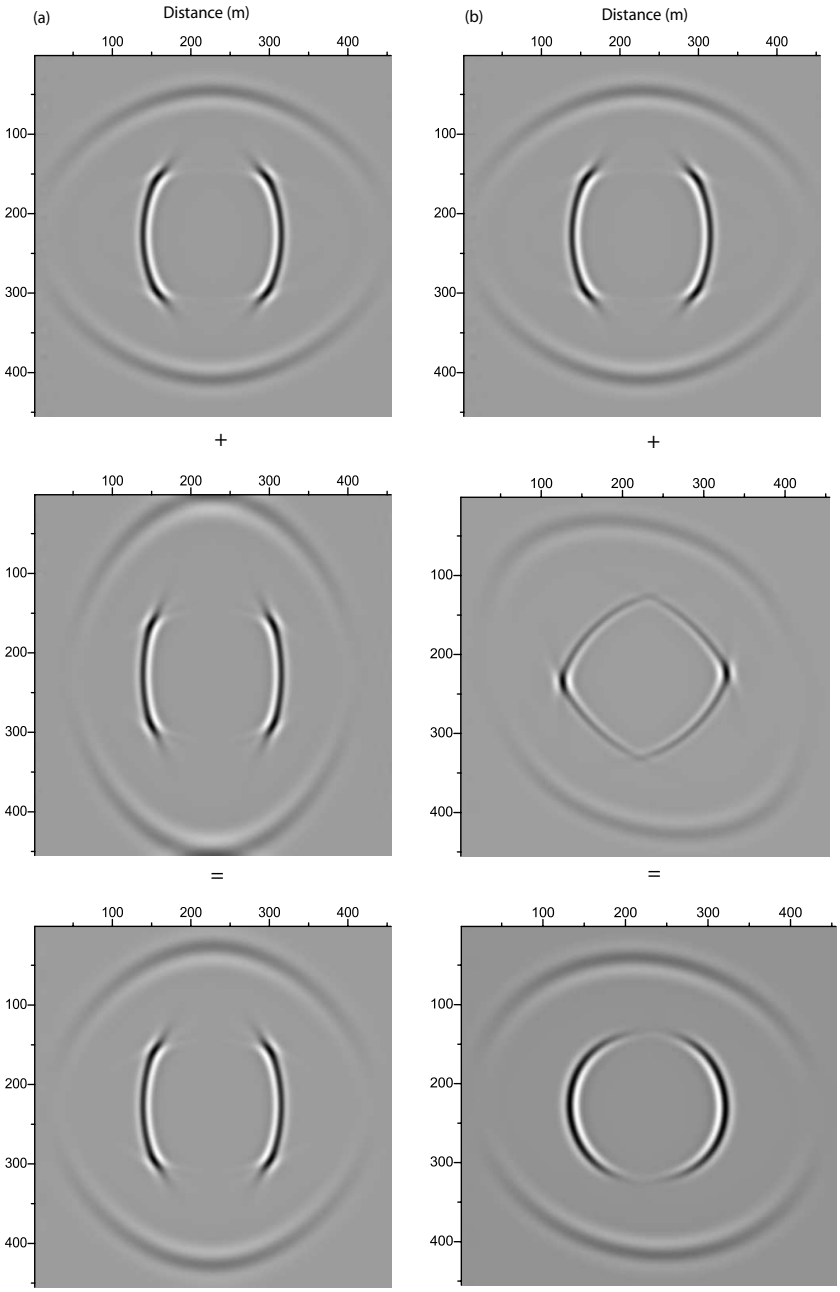

Fig. 3 Snapshots corresponding to the group velocities curves shown in Figure 2. The lower ones refer to the equivalent (Schoenberg-Muir) media.

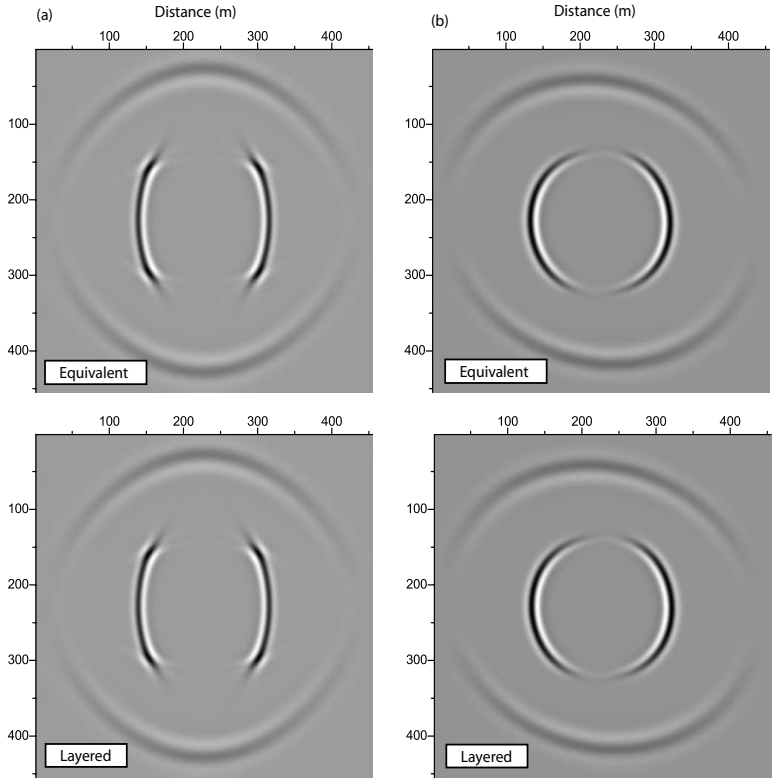

Fig. 4 Snapshots in the orthorhombic (a) and monoclinic (b) effective (Schoenberg-Muir) media (upper panels). The lower panels display the simulations in the finely-layered media. The outer and inner wavefronts correspond to the qP and qS waves, respectively.

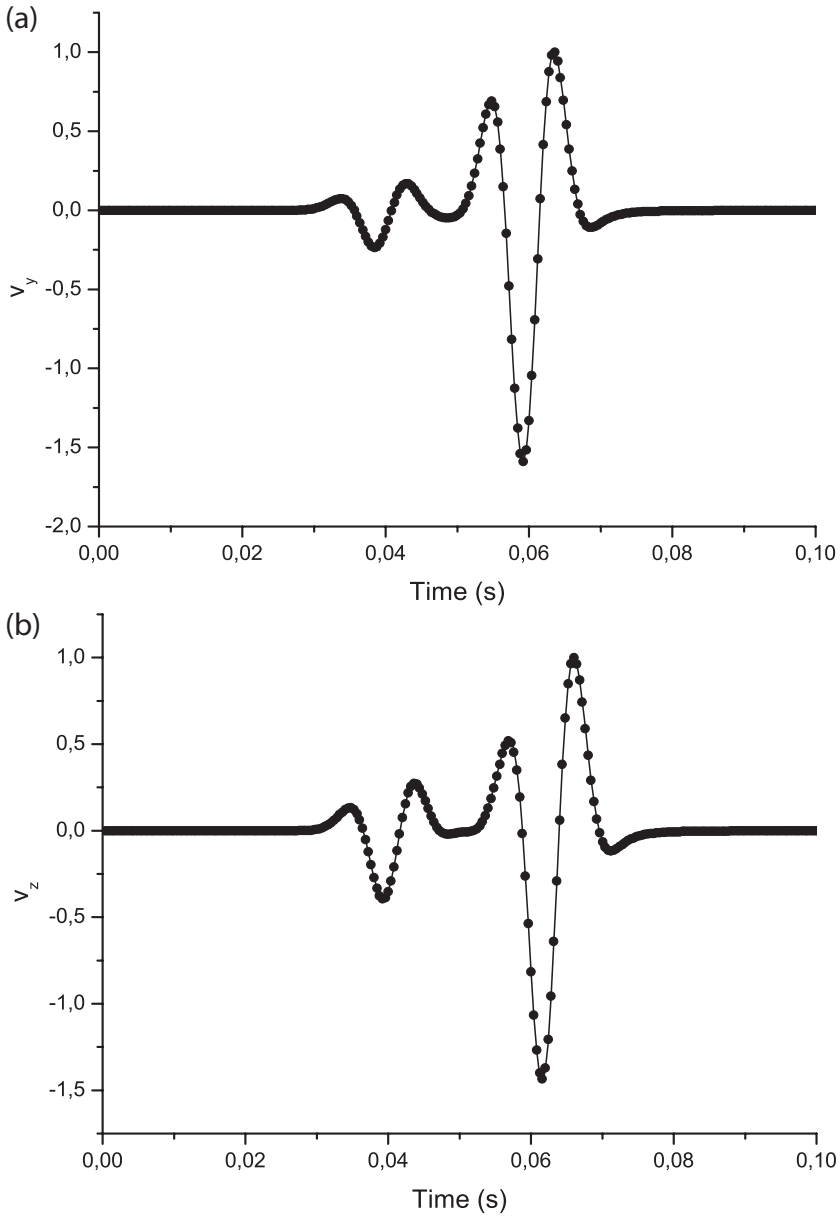

Fig. 5 Time history at $(x, z) = (57, 57)$ m from the source location. The solid line corresponds to the effective (Schoenberg-Muir) monoclinic medium and the dots to the simulations in the finely-layered medium. (a) Orthorhombic medium; (b) Monoclinic medium. The VTI thin layer has 26 % anisotropy.

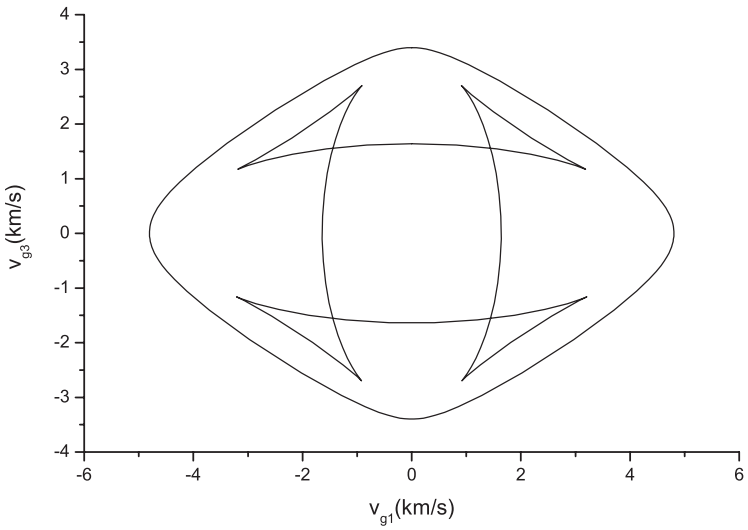

Fig. 6 Group velocity curve corresponding to a strongly anisotropic VTI medium.

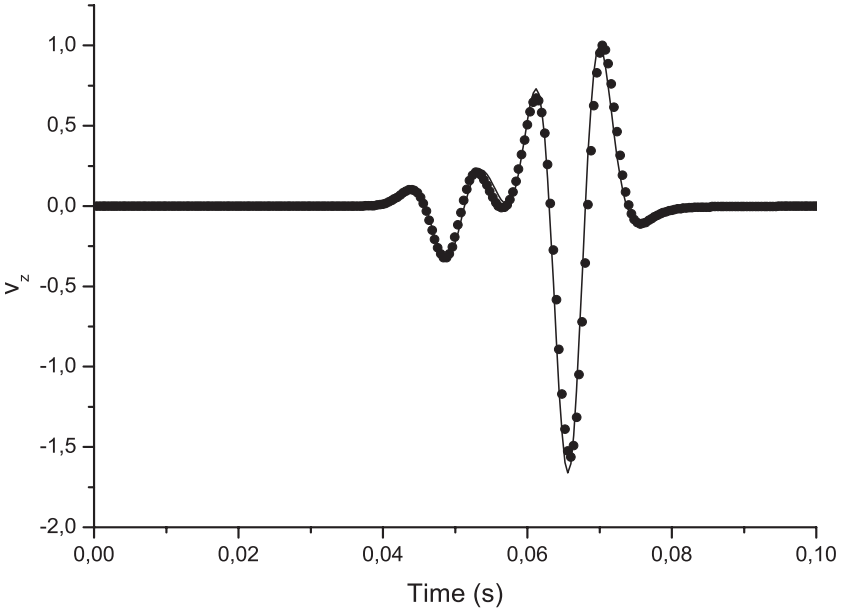

Fig. 7 Time history at $(x, z) = (52, 52)$ m from the source location. The solid line corresponds to the effective (Schoenberg-Muir) monoclinic medium and the dots to the simulations in the finely-layered medium. The VTI thin layer has 50 % anisotropy.